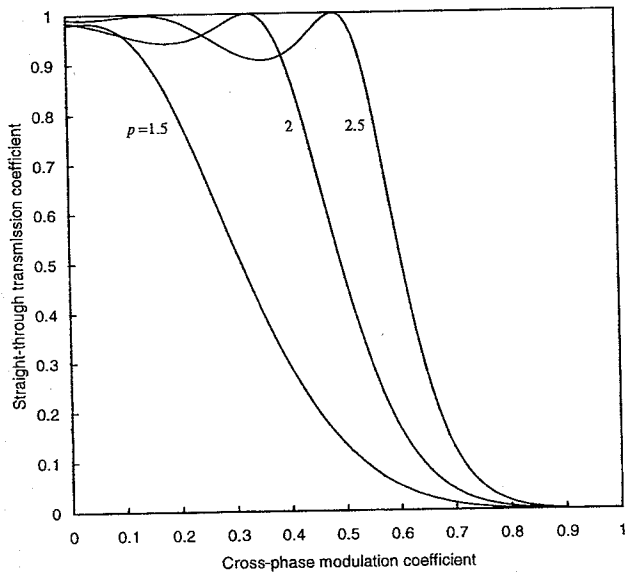

Figure 5 Transmission curves T versus σ with $p = 1.5$, $p = 2$, and $p = 2.5$ for the Lagrangian formulation

required input peak power is easily evaluated with this variational approach (Figure 4). Finally, for a given input peak power, the transmission coefficient, as shown in Figure 5, does not always decrease when the XPM parameter is increased.

REFERENCES

1. S. M. Jensen, "The Nonlinear Coherent Coupler," *IEEE J. Quantum Electron.*, Vol. QE-18, Oct. 1982, pp. 1580–1583.
2. S. Trillo, S. Wabnitz, E. M. Wright, and G. I. Stegeman, "Soliton Switching in Fiber Nonlinear Directional Couplers," *Opt. Lett.*, Vol. 13, Aug. 1988, pp. 672–674.
3. M. Romagnoli, S. Trillo, and S. Wabnitz, "Soliton Switching in Nonlinear Couplers," *Opt. Quantum Electron.*, Vol. 24, 1992, pp. S1237–S1267.
4. M. N. Islam, "Ultrafast Switching with Nonlinear Optics," *Physics Today*, Vol. 47, May 1994, pp. 34–40.
5. F. Kh. Abdullaev, R. M. Abrarov, and S. A. Darmanyan, "Dynamics of Solitons in Coupled Optical Fibers," *Opt. Lett.*, Vol. 14, Jan. 1989, pp. 131–133.
6. F. Abdullaev, S. Darmanyan, and P. Khabibullaev, *Optical Solitons*, Springer-Verlag, Berlin, 1993, Sec. 3.5, pp. 76–80.
7. S. Trillo and S. Wabnitz, "Weak-Pulse-Activated Coherent Soliton Switching in Nonlinear Couplers," *Opt. Lett.*, Vol. 16, Jan. 1991, pp. 1–3.
8. G. P. Agrawal, *Nonlinear Fiber Optics* (2nd ed.), Academic Press, Boston, 1995.
9. P. M. Ramos and C. R. Paiva, "Combined Effect of Cross-Phase Modulation and Higher-Order Dispersion on Soliton Switching in Nonlinear Fiber Couplers," *PIERS'97—Progress in Electromagnetics Research Symposium*, City University of Hong Kong, Hong Kong, Jan. 1997.
10. A. Hasegawa and Y. Kodama, *Solitons in Optical Communications*, Clarendon Press, Oxford, 1995.
11. E. Caglioti, S. Trillo, S. Wabnitz, B. Crosignani, and P. Di Porto, "Finite-Dimensional Description of Nonlinear Pulse Propagation in Optical-Fiber Couplers with Applications to Soliton Switching," *J. Opt. Soc. Am. B*, Vol. 7, March 1990, pp. 374–385.
12. C. Paré and M. Florjanczyk, "Approximate Model of Soliton Dynamics in All-Optical Couplers," *Phys. Rev. A*, Vol. 41, June 1990, pp. 6287–6295.
13. Yu. S. Kivshar, "Switching Dynamics of Solitons in Fiber Directional Couplers," *Opt. Lett.*, Vol. 18, Jan. 1993, pp. 7–9.
14. Yu. S. Kivshar and M. L. Quiroga-Teixeiro, "Influence of Cross-Phase Modulation on Soliton Switching in Nonlinear Optical Fibers," *Opt. Lett.*, Vol. 18, June 1993, pp. 980–982.
15. P. L. Chu, B. A. Malomed, and G. D. Peng, "Soliton Switching and Propagation in Nonlinear Fiber Couplers: Analytical Results," *J. Opt. Soc. Am. B*, Vol. 10, Aug. 1993, pp. 1379–1385.
16. I. M. Uzunov, R. Muschall, M. Göles, Yu. S. Kivshar, B. A. Malomed, and F. Lederer, "Pulse Switching in Nonlinear Fiber Couplers," *Phys. Rev. E*, Vol. 51, March 1995, pp. 2527–2537.
17. A. Ankiewicz, N. Akhmediev, G. D. Peng, and P. L. Chu, "Limitations of the Variational Approach in Soliton Propagation in Nonlinear Couplers," *Opt. Commun.*, Vol. 103, Dec. 1993, pp. 410–416.
18. N. Akhmediev and A. Ankiewicz, "Novel Soliton States and Bifurcation Phenomena in Nonlinear Fiber Couplers," *Phys. Rev. Lett.*, Vol. 70, April 1993, pp. 2395–2398.
19. J. M. Soto-Crespo and N. Akhmediev, "Stability of the Soliton States in a Nonlinear Fiber Coupler," *Phys. Rev. E*, Vol. 48, Dec. 1993, pp. 4710–4715.
20. N. Akhmediev and J. M. Soto-Crespo, "Propagation Dynamics of Ultrashort Pulses in Nonlinear Fiber Couplers," *Phys. Rev. E*, Vol. 49, May 1994, pp. 4519–4529.
21. J. M. Soto-Crespo, N. Akhmediev, and A. Ankiewicz, "Soliton Propagation in Optical Devices with Two-Component Fields: A Comparative Study," *J. Opt. Soc. Am. B*, Vol. 12, June 1995, pp. 1100–1109.

CCC 0895-2477/97

USE OF PML BOUNDARY CONDITIONS FOR WIRELESS TELEPHONE SIMULATIONS

Cynthia Furse, Yan Cui, Gianluca Lazzi, and Om Gandhi
Department of Electrical Engineering
University of Utah
Salt Lake City, Utah 84112

Received 6 January 1997

ABSTRACT: *Previous articles on the perfectly matched layer (PML) boundary condition have focused on the reflections from the boundary itself. This article examines an application of the PML boundary condition to determine if it is preferable to use the PML or the more traditional boundary conditions for finite-difference–time-domain (FDTD) simulations of personal wireless telephones. Retarded time and PML boundary conditions are compared in realistic simulations of cellular telephones operating at 835 and 1900 MHz held against the human head. The peak 1-specific absorption rate (SAR) values, total percent power absorbed, impedance, and radiation patterns are compared, and it is shown that the two boundary conditions provide virtually identical results to within 3% for impedance and 1% for other values, and require similar computer resources. This demonstrates that the PML and retarded time boundary conditions are equally accurate for FDTD cellular telephone simulations and can be used with approximately equal efficiency. © 1997 John Wiley & Sons, Inc.* Microwave Opt Technol Lett 15: 95–98, 1997.

Key words: *finite-difference–time-domain simulation, wireless telephone simulation, bioelectromagnetics*

I. INTRODUCTION

The perfectly matched layer (PML) boundary conditions have been demonstrated to provide significantly less reflection from the boundary than the retarded time or Mur second-

order boundary conditions used for finite-difference–time-domain (FDTD) simulations [1–5]. Although these PML conditions may increase the accuracy of some simulations [6], it has been unclear whether or not they would alter bioelectromagnetic simulation results such as those for wireless telephones. Simulations involving highly absorbing materials may negate the need for PML conditions. Values of interest in wireless telephone simulations include peak 1-g SAR values, total percent power absorbed, and impedance, which are relatively insensitive to the very small reflections from the boundary conditions. In addition, even the radiation patterns of these simulations are relatively forgiving.

This article demonstrates that for wireless phone simulations, retarded time and PML boundary conditions provide peak 1-g SAR values, total percent power absorbed, impedance, and radiation patterns that are equivalent to within 3% for impedance and 1% for all other values. Mur second-order boundary conditions have been previously shown to have error approximately equal to retarded time boundary conditions [4], so this boundary condition is equally effective. Also, all three boundary conditions require comparable computer resources, so all three could be used equally well in FDTD telephone simulations.

II. IMPLEMENTATION OF THE BOUNDARY CONDITIONS

The retarded time absorbing boundary conditions have been implemented as explained in [7]; therefore no further details are given here.

The PML boundary conditions have been implemented following the approach described in [1] and [2]. In this approach, the six field components are split in two components each inside the PML material, leading to 12 coupled equations instead of the original six FDTD equations. As explained in [1], the 12 field components are discretized, with particular attention paid to the interfaces between air and PML material, and the PML region is truncated with perfect electric conductors. Instead of the shape of the conductivity used in [1] and [2], the conductivity in each layer, i, has been chosen independently according to the following formula [4]:

$$\sigma_I = \sigma_0^*((i^{(n+1)} - (i-1)^{(n+1)})/(n+1)), \qquad (1)$$

where n is the order ot the conductivity profile, σ_0 is the conductivity of the first layer, and I is the layer number. This conductivity profile was shown in [4] to provide PML performance that is significantly better than both the retarded time and Mur second-order boundary conditions. For this article the conductivity profile was optimized with the use of the method described in [4] for an FDTD cell size of 1.974 mm. Six layers were used with $n = 3.2$ and $\sigma_0 = 0.01$ S/m.

III. THE TELEPHONE NEXT TO THE HUMAN HEAD

The case of a telephone next to the human head has been studied extensively by several research groups [8–10]. The head model with a resolution of 1.974 × 1.974 × 3 mm used in these simulations was developed at the University of Utah from the MRI scans of an adult male volunteer [13]. Properties of the tissues were provided by Gabriel [11].

The time resolution of the FDTD simulations $dt = \delta/2c = 3.29$ ps was taken to correspond to the smaller of the cell dimensions of 1.974 mm. To ensure converged results, the simulations were run for eight periods of the wave for each of the two frequencies 835 and 1900 MHz analyzed in this study.

A model telephone was developed to represent a possible configuration of representative commercially available phones. It is recognized that various handset dimensions are being used for the cellular telephones, and the dimensions of the handset do influence the radiated fields [12]. We have taken a handset dimension of 2.96 × 5.73 × 15.5 cm, typical of today's handsets. This includes a metal box of dimensions 2.76 × 5.53 × 15.3 cm and a 1-cell thickness of plastic coating. The actual plastic has a thickness $w = 1$ mm, which is thinner than the FDTD resolution, so an effective dielectric constant K_e is used as described in [13]. The antenna is 0.25 wavelength long (9 cm at 835 MHz and 3.9 cm at 1900 MHz), and is also coated with 1 mm of plastic, using the effective dielectric constant.

The 1-g SAR is calculated as described in detail in [8]. According to the ANSI/IEEE C95.1-1992 rf safety guideline for uncontrolled environments, the spatial-peak SAR should not exceed 1.6 W/kg for any 1 g of tissue defined as a tissue volume in the shape of a cube [14]. Because of the irregular shape of the body (e.g., the ears) and tissue heterogeneity, a tissue volume in the shape of a cube of, say, 1 × 1 × 1 cm, will have a weight that may be in excess of, equal to, or less than 1 g. Larger or smaller volumes in the shape of a cube may therefore need to be considered to obtain a weight of about 1 g. Furthermore, for an anatomical model such as the one used in this study with rectangular cell sizes (1.974 × 1.974 × 3 mm), it is not convenient to obtain exact cubical volumes, even though nearly cubic shapes may be considered. We have considered cubes of 5 × 5 × 4 cells to obtain subvolumes on the order of 1 cm^3. For each of these subvolumes selected close to and around the regions of the high SARs, we have divided the absorbed powers by the weights calculated for the individual subvolumes to obtain 1-g SARs. As expected, there is a great deal of variability in the 1-g SARs

TABLE 1 Comparison of PML and Retarded Time Boundary Conditions for 835-MHz Model Phone Test Case. Assumed Radiated Power = 600 mW

	PML (Case 1)	PML (Case 2)	Retarded Time
Absorbed power	321.7 mW	321.0 mW	322.3 mW
Radiated power	278.3 mW	279.0 mW	277.7 mW
Peak 1-g SAR	2.92 W/kg	2.92 W/kg	2.92 W/kg
Peak 10-g SAR	1.09 W/kg	1.09 W/kg	1.09 W/kg
Impedance (ohms)	89.3 + j78.5	89.3 + j78.4	92.1 + j79.0
cpu time (s) (HP755)	47k	28k	28k
Memory for FDTD only (SAR is calculated in postprocessing)	164 Mbytes	101 Mbytes	104 Mbytes

that are obtained. In keeping with the ANSI/IEEE safety guidelines, weights equal to or in excess of 1 g are considered to obtain the spatial-peak SARs given in the tables. A similar method was used to obtain 10-g averaged SARs from a subvolume to $10 \times 10 \times 7$ cells.

Two simulations of the model phone next to the head were made, one at 835 MHz and one at 1900 MHz, and the values of interest are summarized in Tables 1 and 2. For the retarded time boundary conditions, 15 cells were taken between the boundary and the nearest point on the telephone, and 10 cells from other sides of the head to the boundary. For the PML case 1, this same volume was used, with six additional PML layers outside the volume. For the PML case 2, the six PML layers were placed six cells from all points on the head or phone model, creating a smaller FDTD volume. All three methods are in very close agreement for these values of interest.

The radiation patterns of the model telephones next to the head were also calculated with the use of both PML cases 1 and 2 and retarded time boundary conditions. The complex electric and magnetic fields were picked up three cells from the boundaries of the phone and head, and integrated to obtain radiation patterns, which are shown in Figures 1 and 2 for frequencies 835 and 1900 MHz, respectively. The antenna is situated next to the head, as indicated, as if viewed looking down onto the head-and-phone configuration. The location of the antenna is also indicated by the black circle on the phone. The two PML cases give virtually indistinguishable results, and the retarded time boundary condition gives similar results, as well.

IV. CONCLUSIONS

This article demonstrates that the PML boundary condition and the retarded time boundary conditions give very similar results with very similar computer resources for simulations of the human head near a cellular telephone at 835 and 1900 MHz. The peak 1-g SAR values, total percent power absorbed, impedance, and radiation patterns are compared, and it is shown that the two boundary conditions provide results within 1% for SAR and power absorbed, and within 3% for

TABLE 2 Comparison of PML and Retarded Time Boundary Conditions for 1900-MHz Pseudophone Test Case. Assumed Radiated Power = 125 mW

	PML (Case 1)	PML (Case 2)	Retarded Time
Absorbed power	71.8 mW	71.8 mW	72.3 mW
Radiated power	53.2 mW	53.2 mW	52.7 mW
Peak 1-g SAR	1.61 W/kg	1.62 W/kg	1.62 W/kg
Peak 10-g SAR	0.39 W/kg	0.39 W/kg	0.39 W/kg
Impedance (ohms)	$46.7 + j47.7$	$46.7 + j47.7$	$48.1 + j46.0$
cpu time (s) (HP755)	32k	19k	19k
Memory for FDTD only	164 Mbytes	101 Mbytes	104 Mbytes

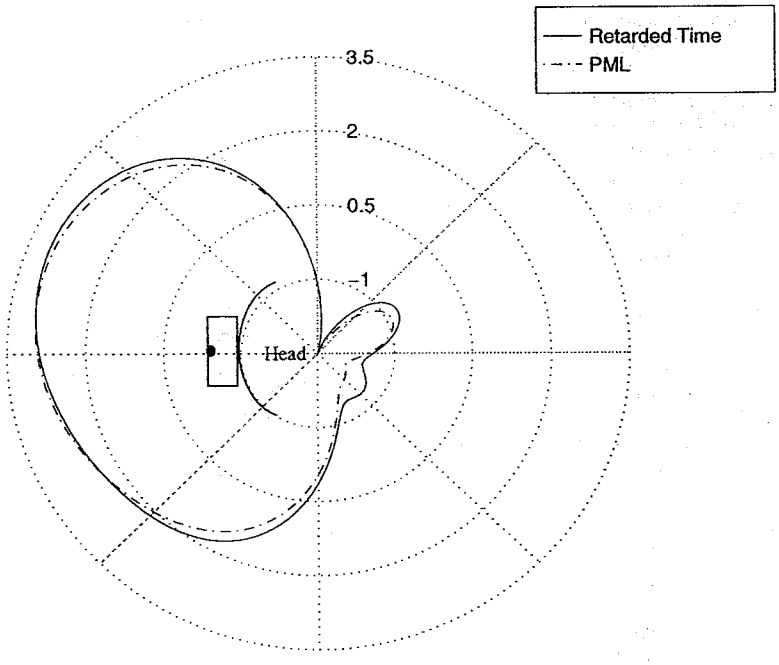

Figure 1 Radiation pattern of a telephone next to a head comparing PML and retarded time boundary conditions for 835-MHz model phone test case

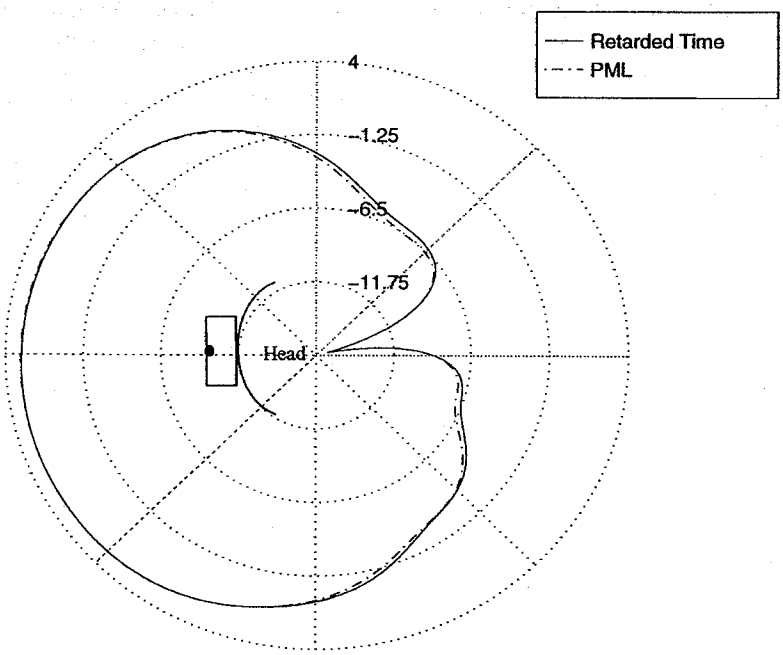

Figure 2 Radiation pattern of a telephone next to a head comparing PML and retarded time boundary conditions for 1900-MHz model phone test case

impedance. This demonstrates that both boundary conditions are equally accurate for FDTD cellular telephone simulations and can be used with approximately equal efficiency.

REFERENCES

1. J. P. Berenger, "A Perfect Matched Layer for the Absorption of Electromagnetic Waves," *J. Comput. Phys.*, 114, 1994, pp. 185–200.
2. D. S. Katz, E. T. Thiele, and A. Taflove, "Validation and Extension to Three Dimensions of the Berenger PML Absorbing Boundary Condition for FD-TD Meshes," *IEEE Microwave Guided Wave Lett.*, Vol. MGW-4, No. 8, 1994, pp. 268–270.
3. W. V. Andrew, C. A. Balanis, and P. A. Tirkas, "A Comparison of the Berenger Perfectly Matched Layer and the Lindman Higher-Order ABC's for the FDTD Method," *IEEE Microwave Guided Wave Lett.*, Vol. MGW-5, No. 6, 1995, pp. 192–194.
4. G. Lazzi and O. P. Gandhi, "On the Optimal Design of the PML Absorbing Boundary Condition for the FDTD Code," *IEEE Trans. Antennas Propagat.*, to be published.
5. J. De Moerloose and M. A. Stuchly, "An Efficient Way to Compare ABCs," *Antennas Propagat. Mag.*, Vol. 38, No. 1, 1996, pp. 71–75.
6. Z. Wu and J. Fang, "Numerical Implementation and Performance of Perfectly Matched Layer Boundary Conditions for Waveguide Structures," *IEEE Trans. Microwave Theory Tech.*, Vol. MTT-43, No. 12, 1995, pp. 2676–2683.
7. S. Berntsen and S. N. Hornsleth, "Retarded Time Absorbing Boundary Conditions," *IEEE Trans. Antennas Propagat.*, Vol. AP-42, 1994, pp. 1059–1064.
8. O. P. Gandhi, G. Lazzi, and C. M. Furse, "Electromagnetic Absorption in the Human Head and Neck for Mobile Telephones at 835 and 1900 MHz," *IEEE Trans. Microwave Theory Tech.*, Vol. MTT-44, No. 10, 1996.
9. M. A. Jensen and Y. Rahmat-Samii, "EM Interaction of Handset Antennas and Human in Personal Communications," *Proc. IEEE*, Vol. 83, 1995, pp. 7–17.
10. P. J. Dimbylow and S. M. Mann, "SAR Calculations in an Anatomically Based Realistic Model of the Head for Mobile Communication Transceivers at 900 MHz and 1.8 GHz," *Phys. Med. Biol.*, Vol. 39, 1994, pp. 1537–1553.
11. C. Gabriel, "Compilation of the Dielectric Properties of Body Tissues at RF and Microwave Frequencies," Final Technical Report submitted to USAF, Occupational and Environmental Health Directorate, Radiofrequency Radiation Division, Brooks Air Force Base, No. AL/OE-TR-1996-0037, June 1996.
12. R. Luebbers, L. Chen, T. Uno, and S. Adachi, "FDTD Calculation of Radiation Patterns, Impedance and Gain for a Monopole Antenna on a Conducting Box," *IEEE Trans. Antennas Propagat.*, Vol. AP-40, 1992, pp. 1577–1582.
13. O. P. Gandhi and C. M. Furse, "Millimeter-Resolution MRI-Based Models of the Human Body for Electromagnetic Dosimetry from ELF to Microwave Frequencies," in P. J. Dimbylow (Ed.), *Voxel Phantom Development*, published by National Radiological Protection Board, Chilton, Didcot, Oxon, 1996, pp. 24–31.
14. ANSI/IEEE C95.1-1992, *American National Standard—Safety Levels with Respect to Exposure to Radio Frequency Electromagnetic Fields, 3 kHz to 300 GHz*, Institute of Electrical and Electronics Engineers, New York, 1992.

CCC 0895-2477/97

A PROPOSED ELECTRO-OPTICAL IMPLEMENTATION OF LATERAL INHIBITION WITH PHASE-ONLY FILTERS

Voula C. Georgopoulos
School of Electrical Engineering and Computer Science
Ohio University
Athens, Ohio 45701

Received 16 December 1996

ABSTRACT: *This article describes a proposed electro-optical implementation of the lateral inhibition function and its simulation. Lateral inhibition is the most important adaptation property in sensory systems*